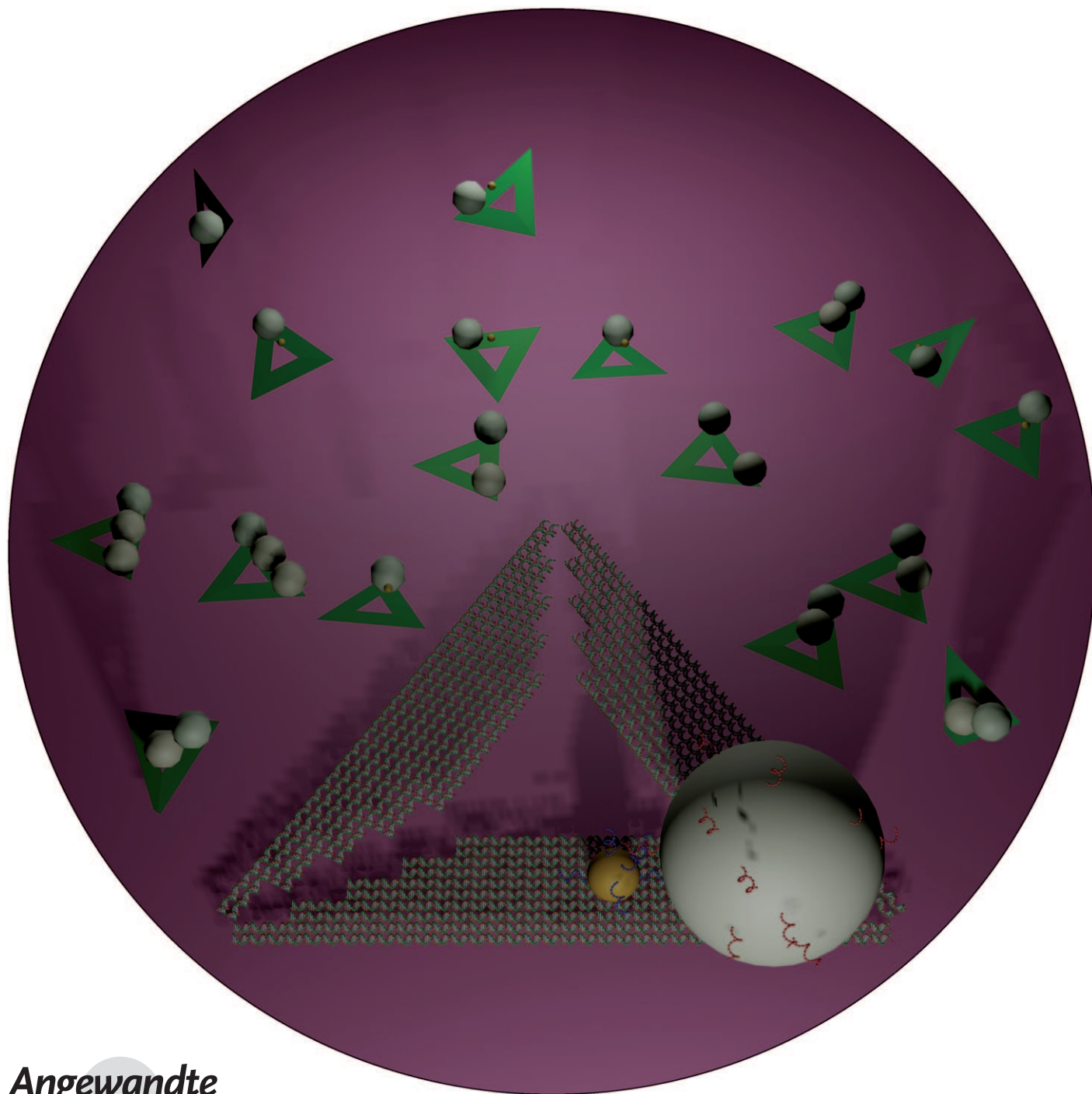


DNA-Origami-Directed Self-Assembly of Discrete Silver-Nanoparticle Architectures**

Suchetan Pal, Zhengtao Deng, Baoquan Ding, Hao Yan, and Yan Liu**



The bottom-up organization of noble-metal nanoparticles (NPs) with nanometer-scale precision is an important goal in nanotechnology.^[1] The DNA-guided self-assembly of these nanoparticles has shown significant progress to meet this challenge.^[2] Enormous progress has been made in the DNA-guided organization of nanoparticles into discrete,^[3] one-dimensional,^[4] two-dimensional,^[5] and three-dimensional architectures.^[6] Facile DNA-functionalization strategies for gold nanoparticles (AuNPs) are now available, making AuNPs preferred (easier) candidates for subsequent self-assembly to form higher-order structures. In contrast, the mediation by DNA self-assembly of the assembly of silver nanoparticles (AgNPs) into higher-order, well-defined discrete nanoarchitectures has not been well explored, mainly as a result of the relative instability of these systems. Ag undergoes oxidation more readily than Au; therefore, the conjugated ligands on the surface of AgNPs are more labile, and AgNPs tend to aggregate irreversibly in solutions with a high salt concentration. However, a high salt concentration is crucial for efficient DNA self-assembly. Recently, we and others started to address this problem by attaching multiple sulfur moieties to DNA^[4c] to form stable AgNP–DNA conjugates that resist aggregation in buffers with a high salt concentration.^[7]

Herein we report a bottom-up method for the fabrication of discrete, well-ordered AgNP nanoarchitectures on self-assembled DNA origami structures of triangular shape by using AgNPs (20 nm in diameter) conjugated with chimeric phosphorothioated DNA (ps-po DNA) as building blocks. Discrete monomeric, dimeric, and trimeric AgNP structures and a AgNP–AuNP hybrid structure could be constructed reliably in high yield. We demonstrate that the center-to-center distance between adjacent AgNPs can be precisely tuned from 94 to 29 nm, whereby the distance distribution is limited by the size distribution of the nanoparticles.

DNA-origami technology^[8] is a well-developed method to create fully addressable DNA nanostructures by using approximately 200 short staple DNA strands to fold a single-stranded genomic DNA (e.g. the DNA of M13mp18, 7249 nucleotides long) into geometrically defined nanopatterns. In this study, we exploited the organizational power of DNA origami to develop a robust strategy for the assembly of otherwise hard-to-control AgNPs into well-defined nano-

architectures. As AgNPs possess unique optical properties (for example, the local surface plasmon resonance (LSPR) effect is stronger between AgNPs than between AuNPs), the strategies demonstrated herein could potentially lead to useful photonic structures enabled by the spatial control of AgNP structures.

AgNPs (20 nm in diameter) were first functionalized with ps-po chimeric DNA strands 9ps-T₁₅, which had a segment of 9 bases with a phosphorothioate (9ps) backbone and a segment of 15 regular DNA bases linked with phosphodiester bonds (T₁₅). The nine sulfur atoms on the ps domain of the DNA backbone provide the DNA strand with high affinity for the surface of the AgNPs (Figure 1 a). When the surface coverage with DNA was at saturation level, the AgNPs showed stability against aggregation in solutions with a high salt concentration (see the Supporting Information and Ref. [7b] for experimental details).

Discrete AgNP architectures were then assembled in a two-step procedure (Figure 1 b). In the first step, a triangular-shaped DNA origami structure^[8] was assembled with the required number of staple strands mixed with three, six, or nine capture strands, each with each a single-stranded overhang of approximately 15 bases that was complementary to

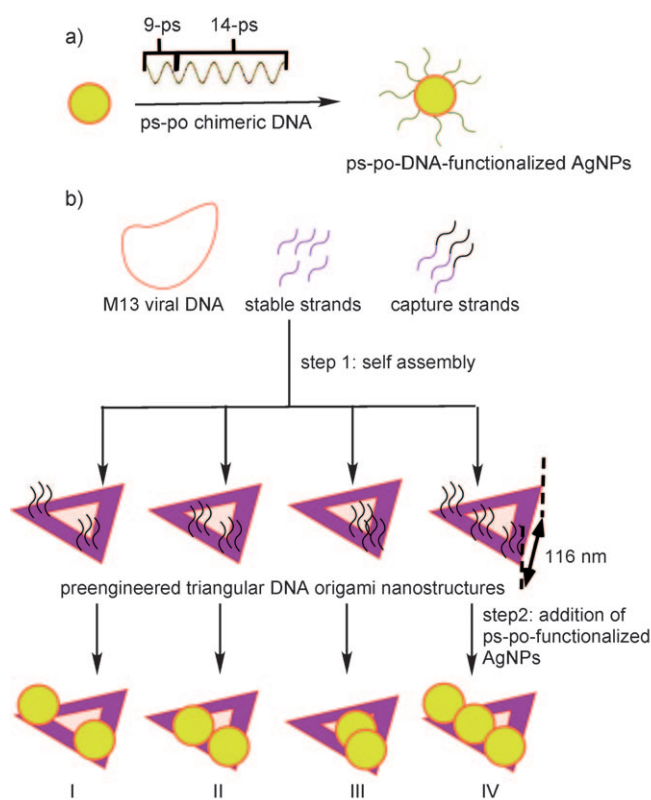


Figure 1. Schematic representation of the fabrication of discrete AgNP architectures by DNA-origami-directed assembly. a) Functionalization of the AgNP with ps-po chimeric DNA. b) Step 1: preparation of preengineered triangular-shaped DNA origami displaying capture strands at predetermined locations on the structure; step 2: hybridization of AgNPs conjugated to ps-po chimeric DNA with capture strands on the DNA origami to form discrete dimeric AgNP architectures (I–III) with different interparticle distances as well as a trimeric architecture (IV).

[*] S. Pal, Dr. Z. Deng, B. Ding, Prof. Dr. H. Yan, Prof. Dr. Y. Liu
Department of Chemistry and Biochemistry and
The Biodesign Institute, Arizona State University
Tempe, AZ 85287 (USA)
Fax: (+1) 480-727-2378
E-mail: hao.yan@asu.edu
yan_liu@asu.edu

[**] This research was partly supported by grants from the ARO, ONR, NSF, DOE, and NIH to Y.L. and from the ARO, ONR, NSF, DOE, NIH, and Sloan Research Foundation to H.Y. Y.L. and H.Y. were supported as part of the Center for Bio-Inspired Solar Fuel Production, an Energy Frontier Research Center funded by the U.S. Department of Energy, Office of Science, Office of Basic Energy Sciences under Award Number DE-SC0001016.

Supporting information for this article is available on the WWW under <http://dx.doi.org/10.1002/anie.201000330>.

the DNA strands on the AgNPs (see the Supporting Information for DNA sequences used). However, the linkage provided by a single hybridized segment of 15 base pairs was not strong enough to hold a particle with a diameter of approximately 20 nm on the origami surface (data not shown). We therefore designed a group of three capture strands arranged in a nearly equilateral triangle approximately 6 nm apart from one another to capture each particle by hybridization to three complementary strands. More than three capturing strands in each cluster, or other arrangements of strands, may create much greater positional uncertainty.

We used A₁₅ as the capture sequence extending from the origami surface and T₁₅ as the sequence on the portion of the chimeric DNA on the AgNP. This choice of sequence ensures a greater degree of freedom for strand hybridization, as it enables possible sliding^[5a] of one single strand against the other to provide enough flexibility for all three capture strands to bind a single 20 nm AgNP simultaneously. In the second step, preengineered DNA origami in different equivalent molar ratios was added to the DNA-functionalized AgNPs in 1x Tris borate/EDTA buffer with 350 mM NaCl (Tris = 2-amino-2-hydroxymethylpropane-1,3-diol, EDTA = ethylenediaminetetraacetic acid) to form the desired structures (see the Supporting Information for experimental details). To ensure that the reaction mixture was sufficiently diluted to limit undesired cross-linking among the discrete structures, we also added 1x Tris acetate/EDTA/magnesium acetate buffer. The mixture was then annealed from 40 to 4 °C to complete the assembly process (see the Supporting Information for experimental details).

The formation of the triangular-shaped DNA origami structures was first verified by transmission electron microscope imaging (TEM) of negatively stained samples (Figure 2a). The length of each arm of the origami was approximately 114 ± 2 nm, which is consistent with the designed length (Figure 1b).

High-fidelity hybridization between capture strands and DNA strands on the AgNPs was verified by using triangular DNA origami that had three capture strands and was designed to capture only one AgNP (Figure 2b). Over 95 % of the triangular DNA origami structures in this sample displayed a single AgNP at one corner (see Figures S3 and S4 in the Supporting Information). Energy-dispersive X-ray spectroscopy (EDS) of these structures showed the presence of silver from the AgNP and uranium from the negative stain (Figure 2c).

To demonstrate the organizational power of our method to create complex AgNP patterns, we further prepared triangular-shaped DNA origami structures displaying capture strands at unique positions to control the assembly of discrete AgNP nanoarchitectures. Three different dimeric AgNP structures, each with well-defined interparticle separations, and an asymmetric trimeric AgNP structure were prepared (Figure 1b, I–IV and Figure 3).

Design I contains two particles at two corners of the triangular DNA origami with a center-to-center distance of approximately 94 nm (Figure 3, Design I). The average distance measured from TEM images of more than 100 of these dimers was approximately 90 ± 3 nm, which is consistent with

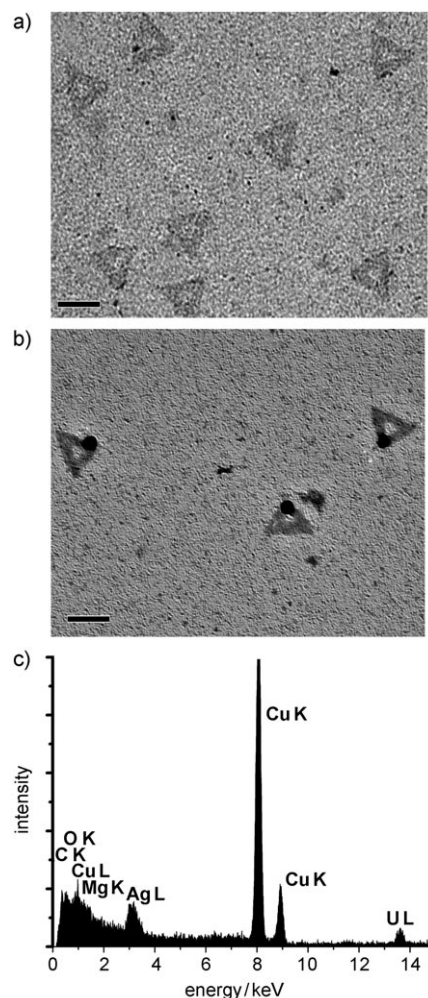


Figure 2. a) TEM image of the triangular DNA origami negatively stained with uranyl formate. b) Hybridization of origami with one AgNP. c) EDS spectrum of the sample in (b) showing the presence of silver from the AgNP and uranium from negative staining. The Cu detected is from the TEM grid. Scale bars on the TEM images: 100 nm.

the designed parameters. The formation of the correct dimer AgNP structure was dominant, with a yield of about 81 %. Since we used two equivalents of the AgNP to the origami structure, a small population of monomeric (12.6 %) and cross-linked structures (7.4 %) was also observed. Design II has an interparticle center-to-center distance of approximately 52 nm by design, with a measured distance of approximately 49 ± 2 nm; the designed dimer structure was formed in similarly high yield (ca. 81 %; Figure 3, Design II). Design III has the shortest center-to-center distance of 29 nm between the two particles by design, and a measured distance of approximately 24 ± 2 nm (Figure 3, Design III). TEM images of this dimer showed a decreased yield relative to the yields observed for the other dimer structures with larger interparticle distances. As the AgNPs have a diameter of approximately 20 ± 2 nm, the measured distance of approximately 24 ± 2 nm indicated that the edge-to-edge distance between the particles was about 4 ± 4 nm. It is possible that the relatively low yield of dimers observed for design III may

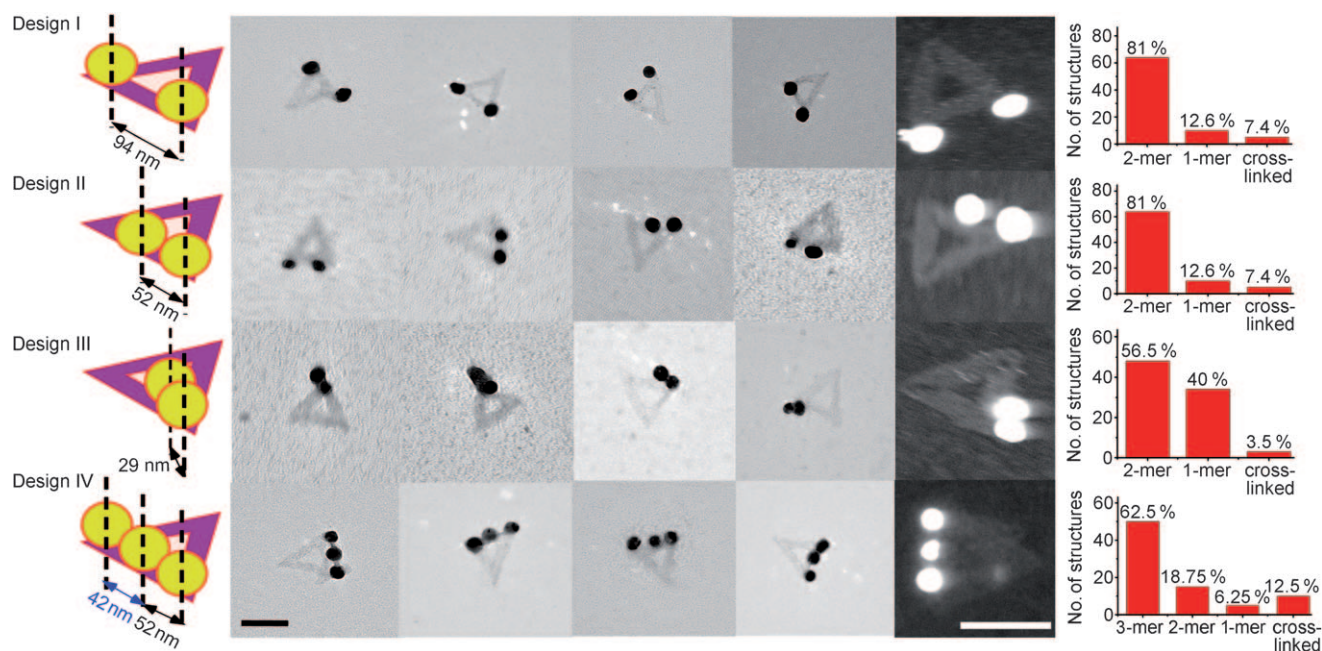


Figure 3. Left: Illustration of individual designs I–IV with different center-to-center distances. Middle: In the first four columns are enlarged TEM images of individual structures after negative staining of the samples with uranyl formate. The shape of the triangular DNA origami can be clearly seen; the dark balls are the AgNPs. The fifth column shows STEM images of the samples without staining. Again, the shape of the triangular DNA origami is clearly visible; the AgNPs appear as bright spots. Scale bars: 100 nm. Right: Yield distribution of the formed structures.

be a result of steric hindrance between the DNA strands on the surfaces of the two approaching particles. As the diameter of the particle is comparable to the distance between the two groups of capture strands, another possibility is that one particle might occupy the space between the two groups and thus prevent the second particle from binding.

We also used a triangular-shaped origami structure with three groups of capture strands on one arm and two different center-to-center distances between neighboring particles: 42 and 52 nm (Figure 3, Design IV). The addition of three equivalents of 9ps-T₁₅-DNA-functionalized AgNPs led to the formation of the desired assembly with an approximately 62.5% yield of the correctly formed trimers. The middle nanoparticle was situated asymmetrically between the other two particles. The measured center-to-center distances of approximately 37 ± 2 and 45 ± 2 nm were about 12% shorter than the designed distances. TEM images showed that the three AgNPs were held on an arm of the origami triangle that was about 10% shorter than the other two arms. We speculate that structural strains caused by the assembly of the three particles on the DNA structure might have caused some distortion of the underlining DNA structure to result in the observed shortening of the triangular triangle arm with the particles attached.

For the designs shown in Figure 3, we also imaged the structure by scanning transmission electron microscopy (STEM; fifth column of images in Figure 3). STEM provides a convenient way to visualize the AgNP-decorated DNA origami samples with high contrast and without any staining. It provided further direct evidence of the assembled structures by showing clearly the AgNPs and the underlining triangular-shaped DNA origami nanostructures.

The organization of different types of noble-metal nanoparticles with control of spatial distance and stoichiometry remains a challenge for bottom-up nanotechnology. In this study, we further demonstrated that DNA origami structures can act as spatial templates for the organization of two different types of nanoparticles through the straightforward assembly of a stoichiometrically controlled heterodimer of an AuNP and an AgNP (Figure 4a). First, we selectively modified a staple strand with a 5 nm AuNP (see the Supporting Information and Ref. [4c] for experimental details). The 5 nm AuNP was first attached to a specific position on the DNA origami structure, in close proximity to the position at which three capture strands (A₁₅) were designed to bind an AgNP. Second, a 9ps-T₁₅-DNA-functionalized AgNP was added in a 1:1 ratio to fabricate the final bimetallic discrete structure. TEM (Figure 4b) and STEM images (Figure 4c) clearly showed the formation of the designed heterodimer structure with an average center-to-center distance of approximately 13 ± 2 nm. EDS analysis (Figure 4d) during STEM imaging of the sample confirmed the presence of both silver and gold elements. The low abundance of Au relative to that of Ag is consistent with the smaller size of the AuNPs.

In summary, the self-assembly of discrete AgNP and AgNP–AuNP nanoarchitectures by using rationally designed DNA templates enabled us to control some of the properties that are essential for hierarchical nanoparticle assembly. These properties include but are not limited to the spatial relationship between the particles and the identity of the particles. The system described herein could potentially be used to gain better insight into particle–particle interactions. Systematic studies with this objective are underway. Although

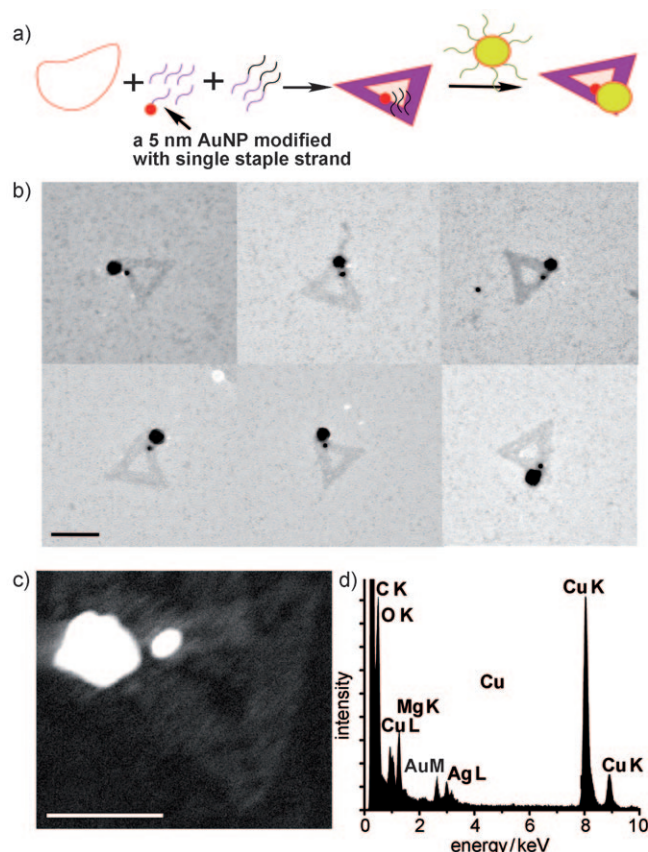


Figure 4. a) Schematic representation of the fabrication of a dimer structure between a 5 nm AuNP and a 20 nm AgNP. b) TEM images of the AgNP-AuNP dimeric structure. Scale bar: 100 nm. c) STEM image of the AgNP-AuNP dimeric structure. Scale bar: 50 nm. d) EDS analysis of the AgNP-AuNP heterodimer on the DNA origami structure.

more systematic investigations (e.g. spectroscopic studies combined with theoretical simulation of the assembled structures) are needed to identify the photonic properties of

the spatially controlled AgNP architectures, we see no fundamental limitation now to the assembly of target structures.

Received: January 19, 2010

Published online: March 16, 2010

Keywords: DNA origami · nanostructures · self-assembly · silver nanoparticles

- [1] M. E. Stewart, C. R. Anderton, L. B. Thompson, J. Maria, S. K. Gray, J. A. Rogers, R. G. Nuzzo, *Chem. Rev.* **2008**, *108*, 494–521.
- [2] C. Lin, Y. Liu, H. Yan, *Biochemistry* **2009**, *48*, 1663–1674.
- [3] For examples, see: a) C. J. Loweth, W. B. Caldwell, X. Peng, A. P. Alivisatos, P. G. Schultz, *Angew. Chem.* **1999**, *111*, 1925–1929; *Angew. Chem. Int. Ed.* **1999**, *38*, 1808–1812; b) F. A. Aldaye, H. F. Sleiman, *Angew. Chem.* **2006**, *118*, 2262–2267; *Angew. Chem. Int. Ed.* **2006**, *45*, 2204–2209; c) J. Sharma, R. Chhabra, C. S. Andersen, K. V. Gothelf, H. Yan, Y. Liu, *J. Am. Chem. Soc.* **2008**, *130*, 7820–7821.
- [4] For examples, see: a) Z. X. Deng, Y. Tian, S. H. Lee, A. E. Ribbe, C. D. Mao, *Angew. Chem.* **2005**, *117*, 3648–3651; *Angew. Chem. Int. Ed.* **2005**, *44*, 3582–3585; b) S. Beyer, P. Nickels, F. C. Simmel, *Nano Lett.* **2005**, *5*, 719–722; c) J. H. Lee, D. P. Wernette, M. V. Yigit, J. Liu, Z. Wang, Y. Lu, *Angew. Chem.* **2007**, *119*, 9164–9168; *Angew. Chem. Int. Ed.* **2007**, *46*, 9006–9010; d) C. M. Niemeyer, W. Bürger, J. Peplies, *Angew. Chem.* **1998**, *110*, 2391–2395; *Angew. Chem. Int. Ed.* **1998**, *37*, 2265–2268.
- [5] For examples, see: a) J. Le, Y. Pinto, N. C. Seeman, K. Musier-Forsyth, T. A. Taton, R. A. Kiehl, *Nano Lett.* **2004**, *4*, 2343–2347; b) J. Zhang, Y. Liu, Y. Ke, H. Yan, *Nano Lett.* **2006**, *6*, 248–251; c) J. Zheng, P. E. Constantinou, C. Micheel, A. P. Alivisatos, R. A. Kiehl, N. C. Seeman, *Nano Lett.* **2006**, *6*, 1502–1504.
- [6] For examples, see: a) D. Nykypanchuk, M. M. Maye, D. van der Lelie, O. Gang, *Nature* **2008**, *451*, 549–552; b) S. Y. Park et al., *Nature* **2008**, *451*, 553–556; c) J. Sharma, R. Chhabra, A. Cheng, J. Brownell, Y. Liu, H. Yan, *Science* **2009**, *323*, 112–116.
- [7] a) J.-S. Lee, A. K. R. Lytton-Jean, S. J. Hurst, C. A. Mirkin, *Nano Lett.* **2007**, *7*, 2112–2115; b) S. Pal, J. Sharma, H. Yan, Y. Liu, *Chem. Commun.* **2009**, 6059–6061.
- [8] P. W. K. Rothmund, *Nature* **2006**, *440*, 297–302.